Trapping and detecting trace radioactive isotopes produced in ICF implosions

Mark Yuly, Stephen Padalino, Adam Brown, Micah Christensen, Micah Condie.

I. Introduction

Several possible designs for a Short-Lived Isotope Counting System (SLICS) are being evaluated using a special test vacuum chamber and "exploding wire" apparatus designed to mimic the conditions present immediately after an Inertial Confinement Fusion (ICF) laser shot. A gas containing a radioactive beta-emitting isotope is rapidly created in the center of the chamber and quickly trapped and counted, simulating outflow of neutral gas in the ICF target chamber and the trapping and detection process.

The long-term objective is to measure light-ion nuclear cross sections at the very low energies of interest for astrophysical phenomena like big bang and stellar nucleosynthesis. These cross sections are usually measured by directing an ion beam from an accelerator into a target and detecting the outgoing product nuclei. At these low energies, however, the cross sections are typically so small that this method would require a difficult and nearly impossibly long accelerator experiment to measure them. In addition, many of the most interesting measurements would require accelerating tritium ions, which would contaminate the beamlines and make the accelerator dangerous to use afterward. In the past these tritium experiments have only been done right before decommissioning the accelerator [1]. For these reasons, most of these reactions, except for the most important and most likely to occur like DT and DD, have never been measured at these energies. Instead, nucleosynthesis calculations rely on cross section extrapolations from measurements made at higher energies. Extrapolating to energies orders of magnitude below measurements, however, is risky and can lead to serious mistakes. For example, in the 1980s S-factor cross section extrapolations made for the $^{2}H(^{2}H, \gamma)^{4}He$ branching ratio were shown to be incorrect by more that seven orders of magnitude at center of mass energies below 25 keV [2]– an observation later found to be due to an unexpected D-state admixture in the ground state [3].

Rather than using an accelerator, a more cost-effective and time efficient way to measure these cross sections may be to use a thermonuclear reaction. This could be done using ICF by doping the target with the desired reactant nuclei, and then trapping and detecting the resultant radioactive products. This has the advantage that counting the decays of the product nuclei occurs much later, in the comparatively quiet environment relatively long after the primary radiation is released. Estimates based on typical OMEGA shot parameters for tritium filled target capsules give yields that may be detectable for a number of reactions, with the highest yields shown in Table 1. A more detailed description of these predictions is in our2018 report [4].

Table 1. Estimated yields for the most prolific light ion reactions that may be studied using ICF. The target capsule was assumed to be doped with 1% of the appropriate reactant isotope. Shot parameters for OMEGA shot 77951 were used, a tritium-filled SiO_2 capsule "exploding pusher" that reached 18.3 keV. For $^{3}H(t,\gamma)^{6}He$ the predicted yield is based on assuming a branching ratio of 10^{-7}, which is simply an estimated "best case". For other reactions, reactivities were calculated using S-factor extrapolations [5] and TALYS-1.9 [6].

Reaction	Product Half-life	Reactant Abundance	Predicted Yield
$^{3}H(t,\gamma)^{6}He$	807 ms	10^{-7} branching	8×10^{4}
$^{6}Li(t,p)^{8}Li$	840 ms	7.6%	$0.2\text{-}1\times10^{7}$
$^{7}Li(t,\alpha)^{6}He$	807 ms	92.4%	$0.7\text{-}2\times10^{6}$
$^{9}Be(t,\alpha)^{8}Li$	840 ms	100%	5×10^{5}

Several possible trap and detector designs are being considered: a turbopump trap detector (described in more detail in our 2019 report [7]), a getter detector (described in our 2017 report [8]) and an ion pump trap for which a prototype has yet to be constructed. Figure 1 illustrates the operation of the turbopump and getter traps. In the turbopump trap on the left, a fraction of the gas atoms leaving the target enter a tube that leads to a turbo pump, which then compresses and traps them in a hollow rectangular plastic scintillator phoswich detector. Radioactive product nuclei in the trapped gas then decay and the resulting beta particles are detected when they strike the walls of the detector. In the getter trap, the product nuclei strike a getter foil, where they either become chemically bound or are implanted. They then decay, and the beta particles are detected by a phoswich detector on the other side of the foil. In both cases, the number of product nuclei entering the trap should be approximately determined by the solid angle of the tube aperture or the getter. In order to measure cross sections using this technique, it is necessary to know the efficiency of the detector trap – that is, if a certain number of product nuclei are produced, what fraction of them are eventually trapped and subsequently detected. One of the main motivations for the experiment described in this report is to explore this question.

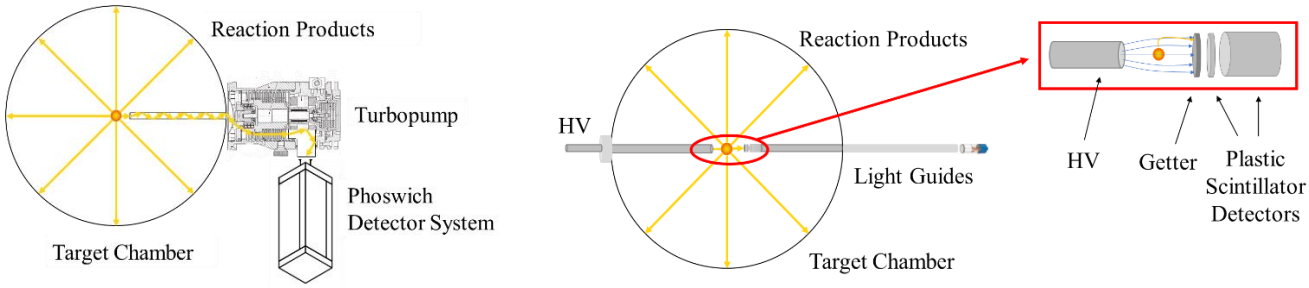

Figure 1. Techniques for capturing and detecting product nuclei. In the turbopump trap (left) the neutral gas containing the product nuclei enters a long tube that directs it into a turbopump. The output port leads the gas to a hollow rectangular phoswich detector where the gas is trapped and product nuclei decays are counted. In the getter trap (right) the atoms containing product nuclei chemically bind to the getter material, and the decays are counted by a small phoswich detector behind the getter. It may be possible to use an electric field to cause inert atoms to implant into the getter.

In order to test this concept under conditions similar to those in an ICF shot, an experiment was designed to simulate the release of a neutral radioactive gas after the laser shot. To create the gas, a tungsten foil electroplated with a thin layer of a material of interest can be activated by bombardment with deuterons or neutrons. In order to achieve good results with the phoswich detectors, the product must beta decay with an endpoint energy of over 1 MeV and preferably not emit gamma rays. Also, to the extent possible, it must meet the mutually exclusive goals of high yield and short half-life. Table 2 shows the best product nuclei that are currently under consideration as test isotopes, and Table 3 shows estimated yields for these products using various likely reactions. The ^{66}Cu nucleus has high yield and some desirable features for a first test, most importantly it will likely stick to the getter, but unfortunately it has a relatively long half-life. Another disadvantage is that natural copper contains both ^{63}Cu and ^{65}Cu, so ^{64}Cu is also usually produced, which emits positrons and therefore emits copious gamma rays. On the other hand, ^{20}F has a much shorter half-life closer to the isotopes in Table 1 but a much lower yield. The product ^{16}N from ^{19}F(n,α)^{16}N also has a short half-life but an even lower yield.

After the coating on the tungsten foil is activated, a large current pulse can be sent through the tungsten to rapidly heat it and vaporize the coating. The gaseous material that is released then can be collected by the traps, and the beta decays counted by the phoswich detectors.

Table 2. Decay properties of ^{16}N, ^{20}F, ^{64}Cu and ^{66}Cu nuclei.

	^{16}N	^{20}F	^{64}Cu	^{66}Cu
Half-life ($t_{1/2}$)	7.13 sec	11.07 sec	12.701 hr	5.120 min
Decay mode	β- (66.2%) Endpoint 4289.2 keV Average 1941.7 keV β- (28.0%) Endpoint 10419.1 keV Average 4979.8 keV	β- (99.99%) Endpoint 5390.86 keV Average 2481.5 keV	β+ (61.5%) Endpoint 653.0 keV Average 278.2 keV β- (38.5%) Endpoint 579.4 keV Average 190.7 keV	β- (9.01%) Endpoint 1601.7 keV Average 628.1 keV β- (90.77%) Endpoint 2640.9 keV Average 1112.1 keV
Gamma rays	6128.6 keV 7115.2 keV	1633.6 keV	511 keV 1345.8 keV	1039.2 keV

Table 3. Rough estimates of the maximum product yield for each of the sources and reactions of interest, assuming infinite irradiation time. Accelerator estimates are based on 10 nA of 3 MeV deuterons. Neutron howitzer estimates assume 10^7 n/s PuBu source a distance of 15.2 cm from the target, with all neutrons moderated to room temperature and no absorption. All targets assumed to be 1 cm^2 by 0.1 mm thick.

Reaction	Target	Source	Max. Yield
^{63}Cu(n,γ)^{64}Cu	Electroplated	Neutron howitzer	6.7×10^5
	Electroplated	Accelerator dd neutrons	7.8×10^5
^{65}Cu(n,γ)^{66}Cu	Electroplated	Neutron howitzer	2.7×10^5
	Electroplated	Accelerator dd neutrons	1.1×10^7
^{63}Cu(d,p)^{64}Cu	Electroplated	Accelerator d	1.5×10^9
^{65}Cu(d,p)^{66}Cu	Electroplated	Accelerator d	1.4×10^8
^{19}F(n,γ)^{20}F	Teflon coating	Neutron howitzer	0.3
	Teflon coating	Accelerator dd neutrons	2.4
^{19}F(n,α)^{16}N	Teflon coating	Accelerator dd neutrons	3300
^{19}F(d,p)^{20}F	Teflon coating	Accelerator d	2.3×10^7

II. Experiment Setup

In order to test the concept of trapping and detecting radioactive product nuclei produced in an ICF shot, a special test vacuum chamber was built [4] and moved from Houghton College to SUNY Geneseo, where it was attached to the downstream side of the 30R beam line scattering chamber on the SUNY Geneseo 1.7 MV tandem Pelletron accelerator, as shown in Figure 2. The 50.8 cm (20 in.) diameter, 15.24 cm (6 in.) high stainless-steel vacuum chamber, shown in Figure 3, has eight 2.75 inch conflat ports around its perimeter and five conflat ports (two 2.75 inch and three 1.33 inch) in a line across the lid. The ion beam produced by the accelerator crossed the 30R scattering chamber, and was transmitted into the test chamber by a short section of beam pipe that included a gate valve that could be used to isolate the test chamber from the rest of the accelerator vacuum system. The turbopump trap was located on the beam left side of the beam-entry port, and the getter trap on the beam right side. Other ports around the test chamber were used for the main chamber pumping Pfeiffer Balzers TPH-062 Turbo Pump with TCP-121 controller, a Duniway I-100-K ion gauge read out by an SRS IGC-100 controller, a Granville-Phillips convectron convection gauge with a GP 275 controller, an SRS RGA100 residual gas analyzer, and an up-to-air valve used to purge the chamber with dry nitrogen.

Figure 2. (Top Left) Houghton Student Micah Condie assembled the computerized valve controls for the turbopump detector at Houghton College prior to moving the chamber to SUNY Geneseo for the experiment. (Top Right) The vacuum chamber was hoisted out of the basement detector lab at Houghton College. (Bottom Left) The chamber and all of the supporting equipment filled a 12-person van. (Bottom Right) Houghton student Micah Christensen reattached the turbopump detector to the vacuum chamber after the chamber was attached to the 30R beam line at SUNY Geneseo.

The feedthrough for heating the tungsten ribbons was inserted through the center port on the lid. A rotation feedthrough in the lid supported an L-shaped aluminum shield that could be positioned between the tungsten ribbon and the getter detector. The purpose of this shield was to prevent beta particles from activated copper that might still be on the tungsten from reaching the getter, since it was desired to see whether copper could be evaporated and then trapped on the getter surface. The shield could also be placed in front of the main turbopump entrance to prevent copper from depositing on the turbopump blades.

A. Valve, Relay and Shield Control System

A control system was constructed to switch the solenoids that control the pneumatic vacuum valves and also the relay that controls the current heating the tungsten ribbon. A control box was made with a manual switch and an MOSFET switch for each valve and the relay. As can be seen in the circuit diagram in Figure 4, when the manual switches are in the on position the valves are opened or the current is allowed through the tungsten filament. When the switches are in

the off position the valves are closed and no current passes through the tungsten, unless they are triggered externally using the MOSFETs. This automatic mode is made possible by a cable connecting the control box to an external MOSFET board controlled by an Arduino Mega. The Arduino serves a webpage using an ethernet shield that allows the switching to be controlled remotely from a safe distance using the same private network used for data acquisition using the FemtoDAQ..

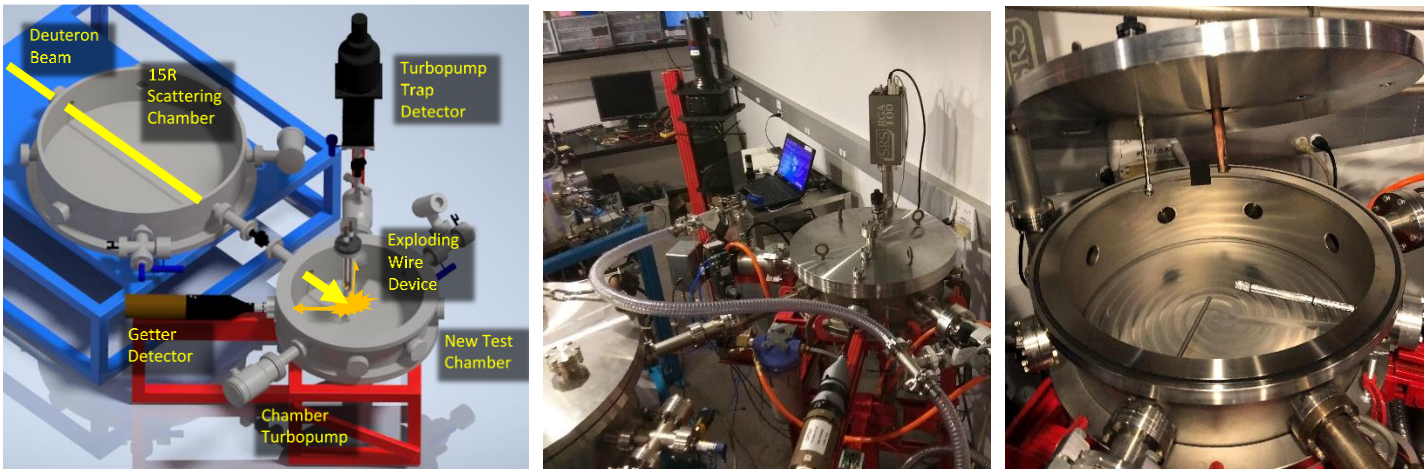

Figure 3. (Left) CAD drawing of SUNY Geneseo Pelletron 30R beamline, showing the attached test chamber and detectors to scale. The beam enters through the indicated port and activates the copper coated tungsten target. The target heats up, evaporating the copper with is then trapped and detected. (Center) Photograph of the test chamber attached to the 30R scattering chamber. (Right) The test chamber with the lid lifted to view the turbopump collection tube, the foil wrapped getter detector and light guide, and, attached the lid, the tungsten ribbon heater feedthrough and the rotating shield.

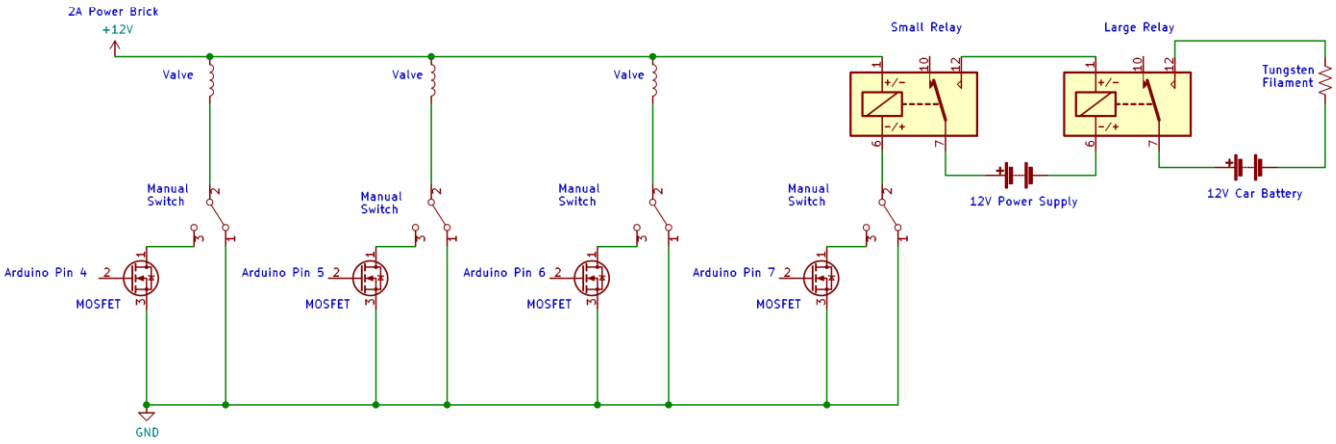

Figure 4. Schematic diagram of the circuit used to control the vacuum valves and heat the tungsten ribbon. The circuit allows for manual control using switches on the control box as well as remote control using an Arduino web server on a private network.

The Arduino also can use used to remotely control the position of the shield attached to the rotation feedthrough. The shield will rotate between the getter detector and the tungsten filament shortly after the “explosion”. This reduces beta counts coming from any remaining activated copper on the filament only a few centimeters away. Since the shield needs to change position shortly after the wire “explodes” it may not be safe to be near enough to the chamber to turn the rotation feedthrough knob, so a servo motor was attached to the top of the rotary feedthrough knob using 3D

printed plastic parts. The servo motor is controlled by one of the PWM pins on the Arduino Mega. The position of the shield can also be changed through the webpage served by the Arduino and ethernet shield.

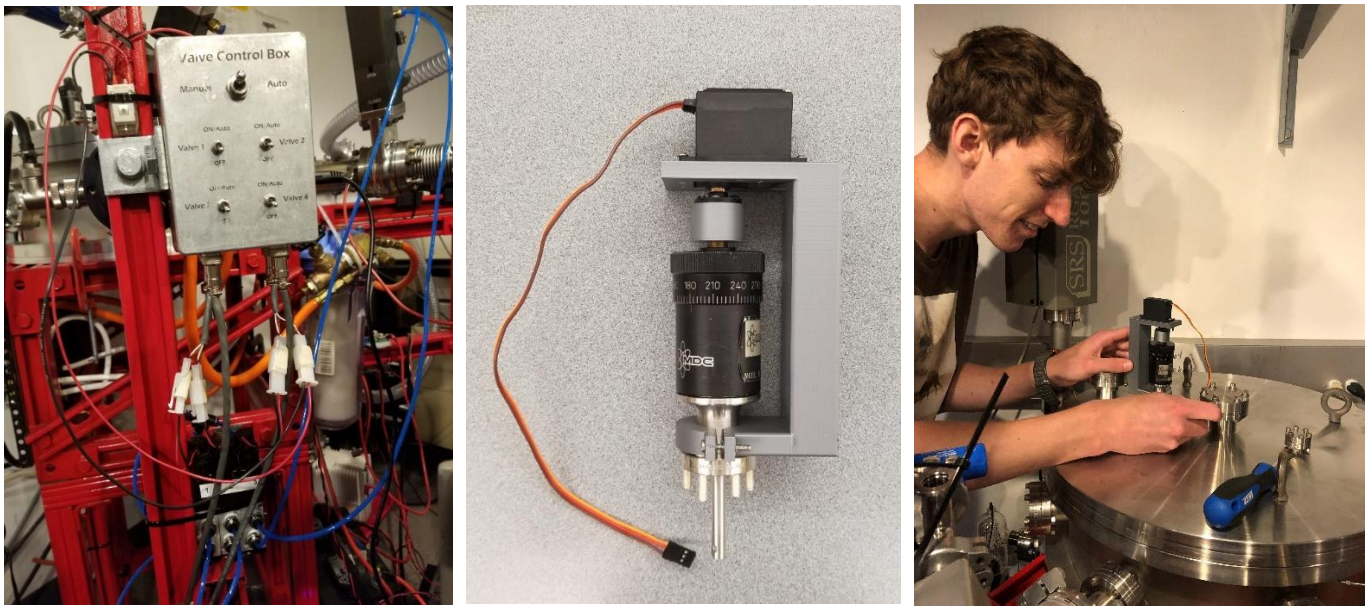

Figure 5. (Left) Valve and tungsten ribbon heater control box. The pneumatic solenoid valves are below with blue tubing. (Center) The homemade servomotor-powered rotary motion feedthrough used for moving the shield. (Right) Houghton student Micah Condie installing the rotary feedthrough on the vacuum chamber.

B. Getter trap and detector.

The getter trap itself was tested in several previous experiments (see 2017 [8] and 2018 [9] reports) but with the plastic scintillator phoswich detector optically coupled directly to the phototube rather than though a light guide. In order for the detector to bring the detector a few centimeters from the target, a lightguide that penetrated into the vacuum chamber was needed. The detector, shown in Figure 6, consists of a 1 mm thick, 9.5 mm (3/8 inch) diameter fast EJ-212 scintillator optically coupled using EJ-500 optical epoxy to a 15 mm long, 10 mm diameter cylinder of slow EJ-240 scintillator. This assembly is coupled using EJ-500 optical epoxy to a 45.9 cm long, 10.1 mm diameter glass optical fiber lightguide which was held firmly against a Burle 7585 phototube by set screws in a 3D printed plastic holder. The optical coupling between the lightguide and phototube was made using EJ-550 optical silicone grease. A vacuum seal is made possible using a #110 Viton O-ring compressed against the glass and a special aluminum 2.75 inch conflat flange. The light guide was covered with aluminum foil to reflect stray light back into the lightguide, and the part outside the vacuum chamber was mad light tight using black plastic tape.

In order to determine the best lightguide material, acrylic, polycarbonate, and glass fibers were all tested. A 1 mm thick EJ-212 scintillator and an RCA 7585 phototube were optically coupled to the ends of each lightguide using optical grease, a 1 μCi ^{241}Am source was then placed against the plastic scintillator, and the entire assembly was made light tight. The ^{241}Am source emits approximately 5 MeV alpha particles, which produce light pulses of approximately all the same size. This light is attenuated by traveling through the light guide, and can be lost out the sides of the light guide, so that much less light reaches the phototube. Table 4 shows the transmission of light reaching the phototube that was converted to an electrical pulse, as a fraction of the amount without the light guide. This was measured two ways, by directly comparing the size of the signal pulses using an oscilloscope, and by measuring the location of the peak in the pulse height spectrum recorded using a multichannel analyzer.

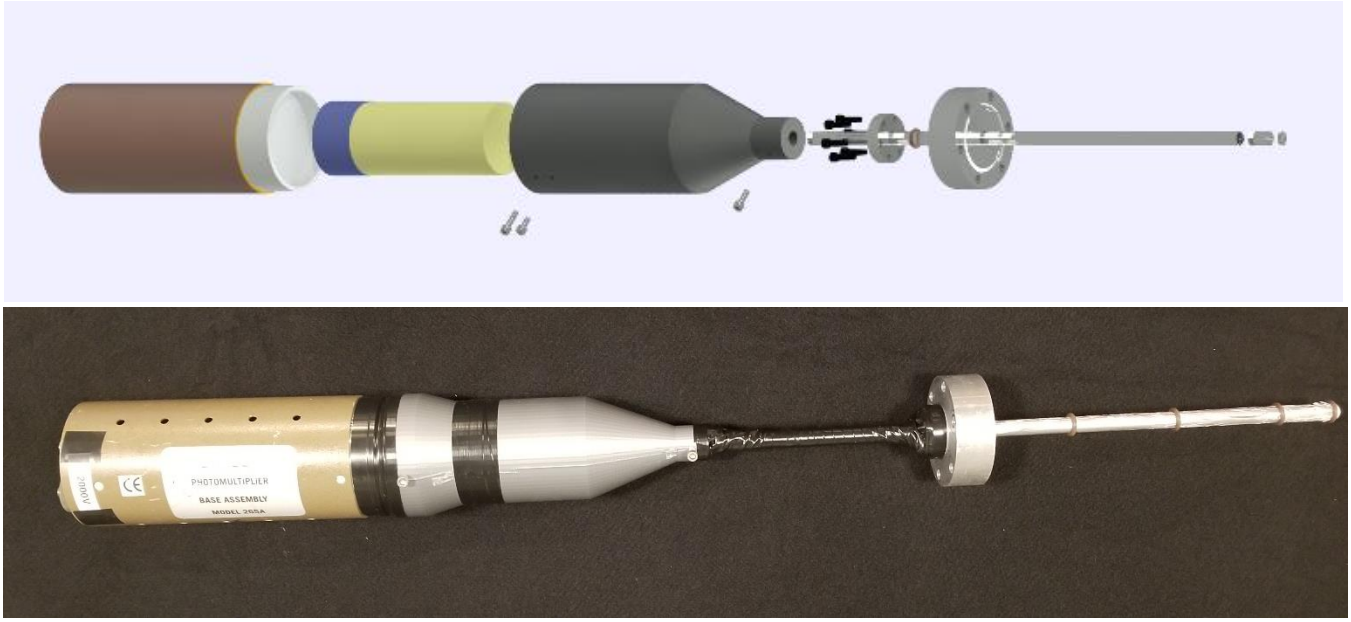

Figure 6. (Top) CAD drawing of the getter detector, showing how the dE and E detectors are attached to the end of the glass light guide. The vacuum seal is obtained using a Viton O-ring pressed against the glass rod and the home-made aluminum conflat flange. The 3D print plastic holder presses the other end of the light guide against the photomultiplier tube face. (Bottom) A photograph of the completed detector, covered with reflective aluminum foil and made light tight outside the vacuum chamber.

Table 4. Transmission of light for different lightguide materials, with and without an aluminum foil reflector.

Material	Length (cm)	Diameter (cm)	Transmission (Foil)	Transmission (No Foil)
Glass	45.9	1.01	42%	32%
Acrylic	46.0	0.91	29%	22%
Polycarbonate	46.0	0.91	0%	0%

Because the phoswich detector system works by separating the fast and slow parts of the PMT signal electronically, the shape of the signal is very important. When so much light is lost in the light guide the shape is affected – in particular, the long tail of the pulse becomes "noisier" due to fluctuations caused by individual photons striking the photocathode. For this reason, as shown in Figure 7, two 2-inch phototube models were tested, a Photonis XP 2262 and a Burle 7585. Clearly, the Burle 8575 phototube had a smoother signal, especially in the long tail of the pulse created by the slow plastic scintillator. In addition, the short pulses in the thin plastic scintillator seemed to be widened and misshapen when they were large in the XP2262.

C. Turbopump trap and detector

The turbopump trap and detector was build and tested in 2019, as described in detail in the 2019 report [7]. It is a roughly 4π solid angle detectors consisting of a hollow 246 x 84 x 84 mm outside dimension box made of plastic scintillator. The outer, 18 mm thick layer is EJ-240 slow plastic scintillator, which is lined with a 1 mm thick layer of EJ-212 fast plastic scintillator. Light from all the scintillators is collected by a 130 mm (5-inch) phototube attached to one end. In the other end is a QF16 flange that can be used to connect the detector to the output port of the Edwards EXT70H Turbo pump using a BOC Edwards EXC120 controller. The inlet of this turbopump trap is a 6.35 mm (0.25 inch) OD diameter, 0.254 mm (0.010 inch) wall thickness 316L stainless steel tube that leads to approximately 3 cm from the center of the chamber.

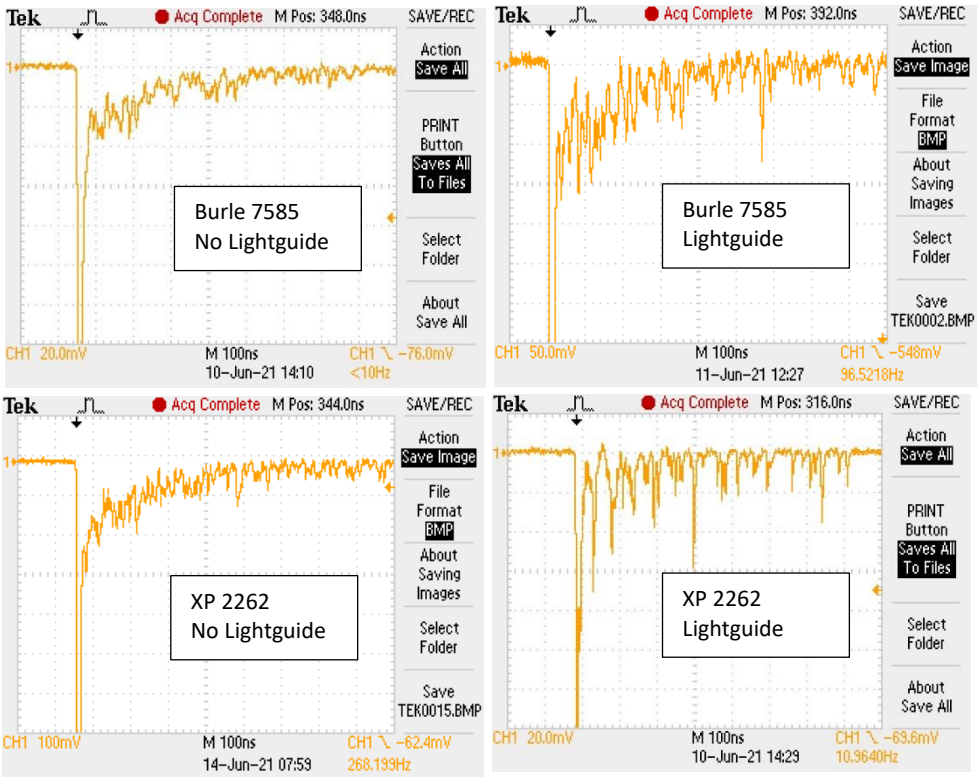

Figure 7. Comparison of PMT pulses from a 0.1 μCi ^{207}Bi source and a 10 cm diameter phoswich detector with the Burle 7585 (top) and Photonis XP2262 (bottom) phototubes, with (right) and without (left) the glass light guide. The Burle 7585 seemed to show superior performance.

Two photomultiplier tubes were tested, an ADIT B133D01 with the homemade base described in the 2019 report [7] and an ET Enterprises 9823KB using the manufacture's recommended base. A 10 cm diameter phoswich detector, similar to the one used for the getter detector, was optically coupled to the center of each phototube using EJ-550 optical grease, and a 0.1 μCi ^{207}Bi source was placed on top. As can be seen in Figure 8, the ADIT B13D01 tube had a much smoother signal, especially for the tail from the slow scintillator. The 9823KB tube did seem faster (for example, the fast scintillator peak was somewhat narrower) but that was deemed of less importance than the slow signal for this application, so the ADIT tube was used.

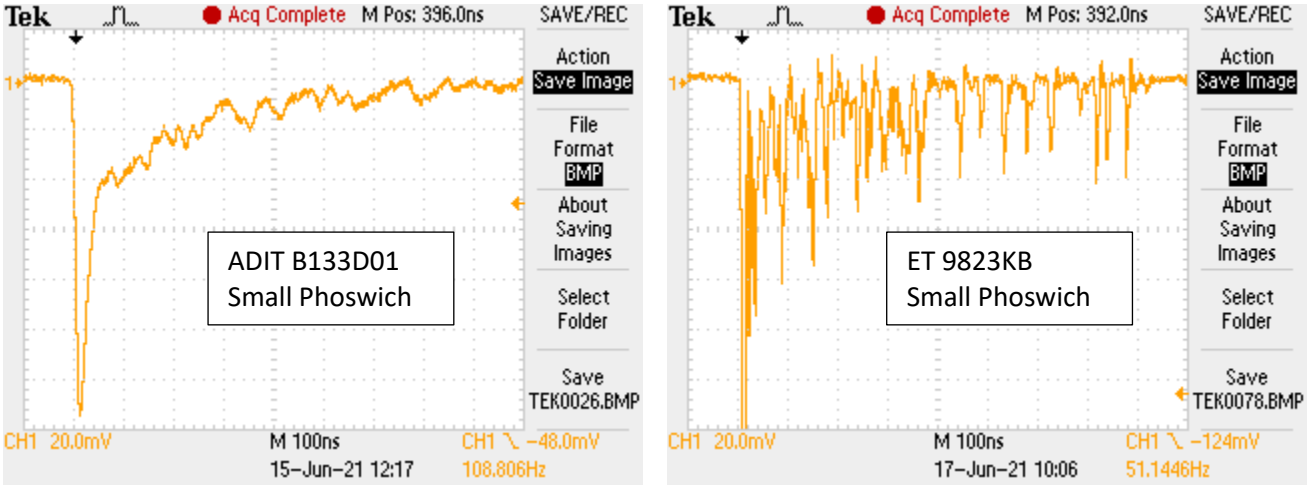

Figure 8. Comparison of PMT pulses from a 0.1 μCi ^{207}Bi source and a 10 cm diameter phoswich detector with the ADIT B133D01 (left) and ET 9823KB (right) phototubes. The ADIT B133D01 seemed to show superior performance.

D. Electronics

Because of the sizable light attenuation in the light guide, the old ORTEC LG105/N linear gate and stretcher modules no longer were adequate. These modules "stretch" the largest voltage occurring within the gate. Large fluctuations, especially in the tail, meant that the value that was "held" by the linear gate and stretcher was no longer proportional to the true pulse height (which itself should depend on the integral of the pulse current, in other words, the total charge collected). Instead, the value simply represented the largest voltage noise spike within the gate.

In order to remedy this, the circuit was changed to use Phillips 7415 linear gates. This linear gate, which does not include a "stretcher" circuit, simply transmits the input single to the output for the duration of the gate. As can be seen in the block diagram in Figure 9, the linear gates select the appropriate part of the input pulse (i.e. either the fast pulse from the dE scintillator or the slow tail from the E scintillator) and passes it to the ORTEC 454 Fast Filter Amplifier, which then integrates and amplifies the signal – giving a output proportional to the energy lost by the particle in the scintillator plastic. The disadvantage of the Phillips 7415, however, is that it is a CAMAC module rather than NIM, so it requires a separate CAMAC crate just for the single module.

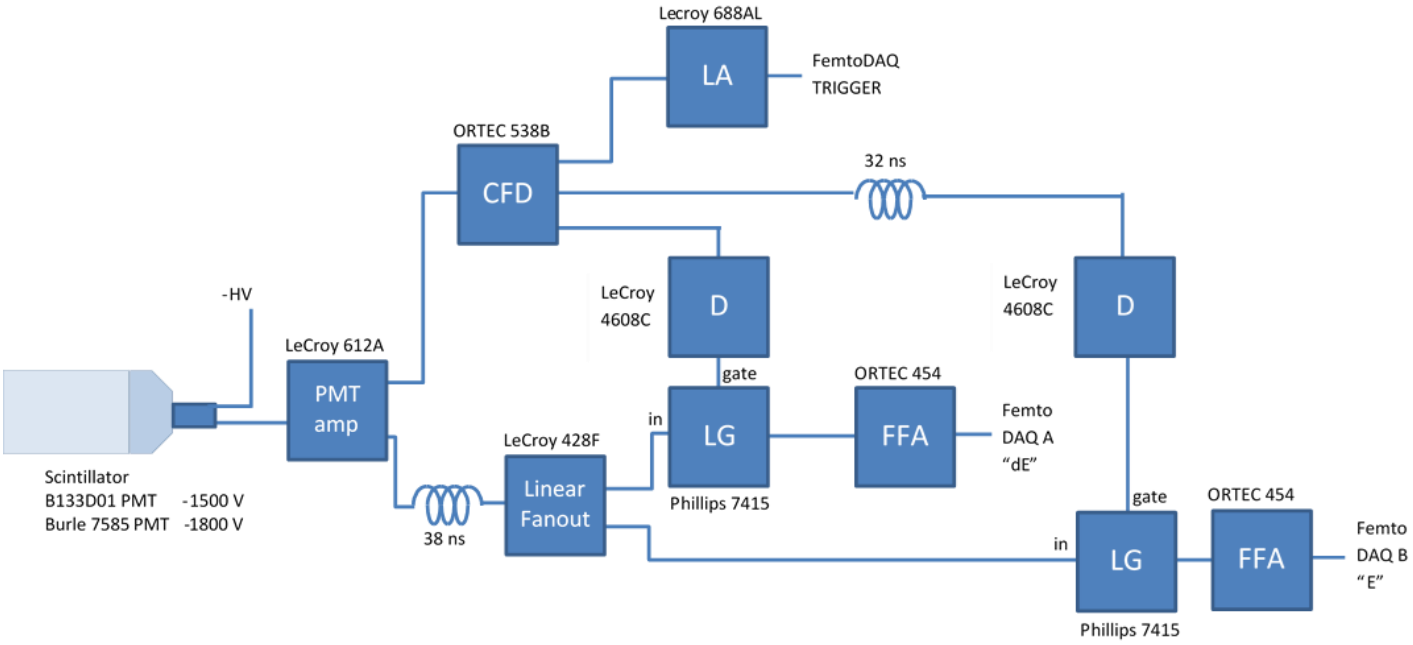

Figure 9. Block diagram of the electronics for analyzing and digitizing the pulses from the phoswich detector. Pulses from the phoswich detector phototube are first amplified (PMT amp), then the signal is split (Linear Fanout) and input to two linear gates (LG). These two linear gates are gated by a logic pulse from the constant fraction discriminator (CFD), which also triggers the FemtoDAQ to digitize. The discriminators (D) simply adjust the width of the gating logic pulse, and the delays select the appropriate times for the logic pulses in order to separate the dE and E signals. Finally, the fast filter amplifiers (FFA) integrate the selected pulses to obtain the best possible resolution.

E. Target Foils

The apparatus for heating the tungsten ribbon, shown in Figure 10, was built and tested by students from SUNY Geneseo and is described more fully in their report. The 0.05 mm thick tungsten ribbons are approximately 6.5 x 12.5 mm strips, spanning the distance between the thick copper electrodes on the feedthrough. Copper, electroplated on the center of the foil, is rapidly evaporated when a pulse of approximately 100 A travels through the foil for several seconds. This current is switched using a high current relay from an automobile and supplied by an automobile battery. The relay itself is switched using a smaller relay which can be energized using a MOSFET power amplifier switched by one of the GPIO outputs of the Arduino controller that is used to remotely control the vacuum valves.

Figure 10. (Left) Copper and tungsten electrodes submerged in $CuSO_4$ solution for electroplating. (Center) Vacuum feedthrough used for heating the tungsten ribbon. (Right) Copper plated tungsten ribbon glowing while being heated in the vacuum chamber. Since the ribbon surface is facing in the direction of the getter detector, this photograph is the uncoated back of the ribbon. The end of the collection tube for the turbopump trap is coming in from the right.

The copper is electroplated onto the tungsten ribbon using a saturated copper sulfate solution. First the electrodes are prepared by roughening the surface with 400 grit emery cloth followed by cleaning with distilled vinegar and rinsing with DI water. Approximately 200 g of $CuSO_4$ are stirred into 800 mL of distilled water until almost all of the crystals dissolve. The copper and tungsten electrodes are suspended in the solution using alligator clips, and a fixed current of about 1 A is allowed to pass between them. The voltage required to produce this current starts at about 3.3 V, then eventually increases to 3.9 V in the course of a typical electroplating process.

III. Neutron Howitzer experiments

Prior to obtaining the deuteron beam, several measurements were carried out using the SUNY Geneseo PuBe neutron howitzer. Inside the howitzer a ^{239}Pu source emits alpha particles which then interact with ^{9}Be to produce neutrons via the $^{9}Be(\alpha,n)^{12}C^*$ reaction. These are fast neutrons, with an energy spectrum reaching up to as high as 10 MeV. These neutrons slow down in the water shielding of the howitzer where they become thermalized and eventually are captured.

For the current experiment, copper foils, of varying thickness from 0.0125 mm (0.0005 inch) to 0.1 mm thickness and approximately 5 cm x 5 cm square, were suspended in plastic bags by strings in the shielding water of the howitzer, about 15.2 cm from the source. The thermal neutrons have very large cross sections for activating copper: about 5 barns for the $^{63}Cu(n,\gamma)^{64}Cu$ reaction and 2 barns for $^{65}Cu(n,\gamma)^{66}Cu$. Since the half-life of ^{64}Cu is 12.7 hours, it was possible to activate the copper at SUNY Geneseo and then bring it to Houghton. where the ^{64}Cu was used to test the detectors. To do this, the copper foils were activated for about five ^{64}Cu half-lives, then driven to Houghton, rolled into a tube, placed inside the turbopump detector, and counted for approximately two half-lives (24 hours). The ^{66}Cu produced at the same time, which has a half life of only 5.12 min., would have long since decayed by the time the foil reached Houghton.

Figure 11 shows the best fit decay and growth curves for all events. For this case, the decay fit gave 15.5 ± 1.0 hr. and the growth fit gave 11.3 ± 0.1 hr. The reason for the difference from the expected 12.7 h half-life has not been determined.

Once the detector system was brought to SUNY Geneseo, it became possible to measure the decay curve for ^{66}Cu, since it only took a few minutes to transfer the activated sample from the howitzer to the detectors. A 0.1 mm thick, approximately 1 cm square of copper was activated in the howitzer for 30 minutes then inserted into the center of the turbopump detector or fixed approximately 2 cm from the front face of the getter detector and counted for 30 minutes. Figure 12 shows the 2D histograms and growth curves obtained for each detector. A fit to the growth curves gave a best

fit decay constant of 0.00223 ± 0.0005 s^{-1} (half-life of 5.19 min.) for the getter detector and of 0.00227 ± 0.0002 s^{-1} (half-life of 5.09 min.) for the turbopump detector, as compared to the published value of 5.12 min.

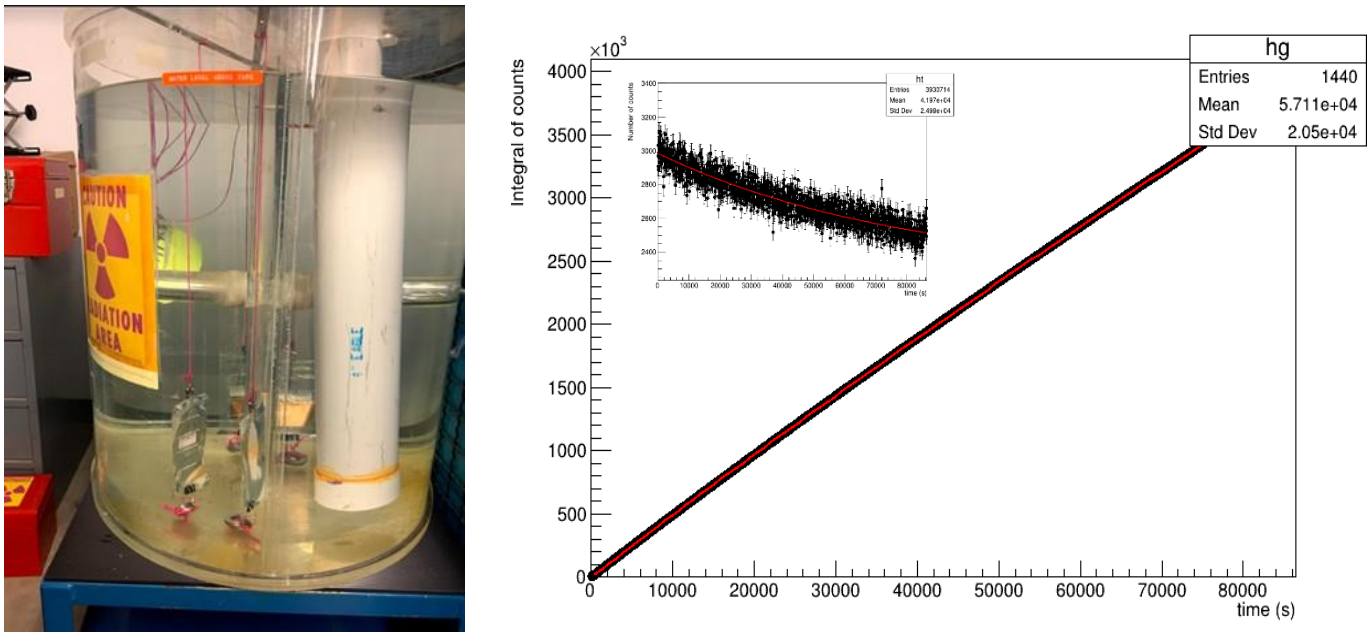

Figure 11. (Left) PuBe neutron howitzer with copper samples suspended from strings in the shielding water. (Right) Decay (inset) and growth curves produced for all events detected by the turbopump phoswich detector in 24 hours of counting. The red curve is the best fit to a decay or growth curve, respectively, plus background.

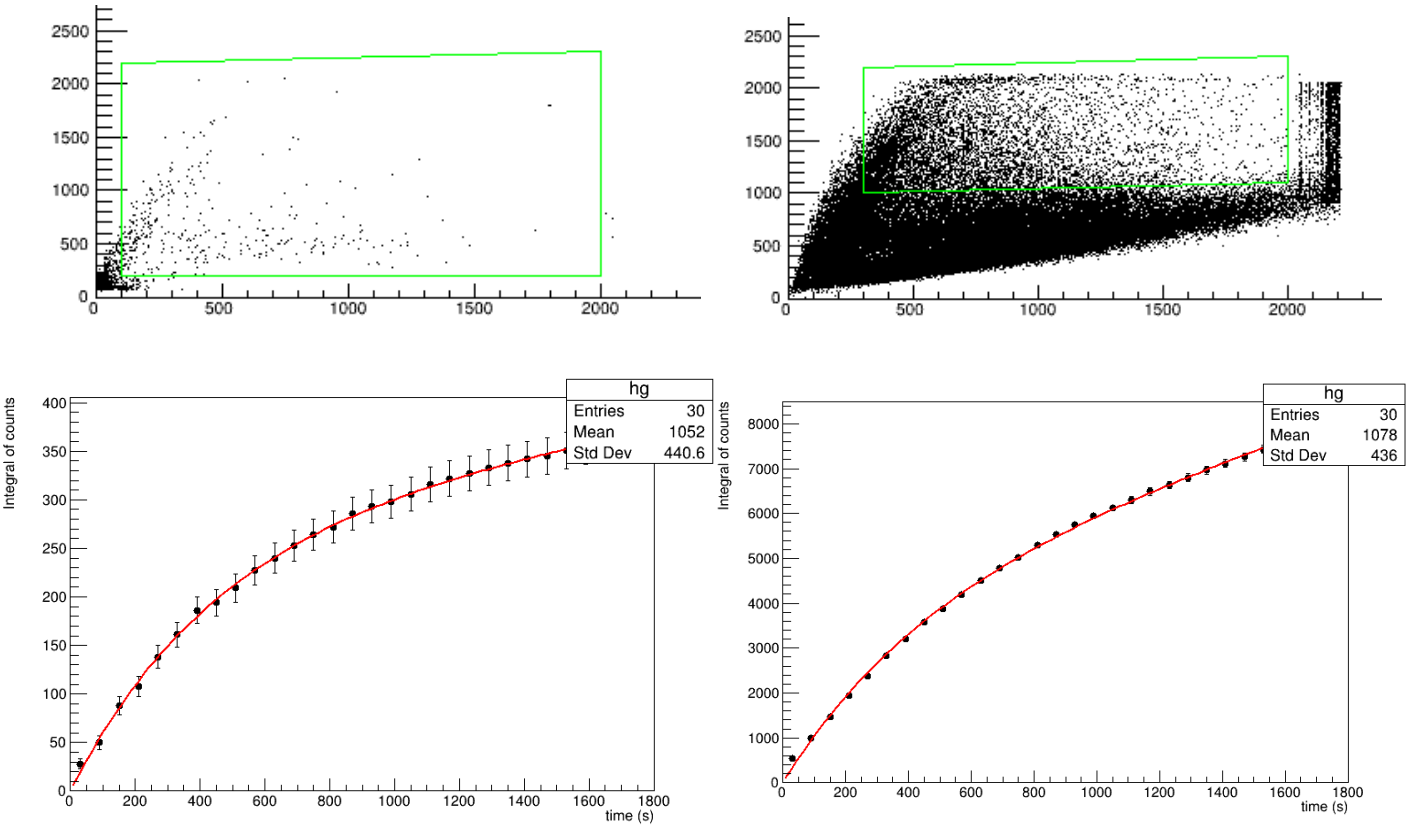

Figure 12. (Left side) The dE-E 2D particle identification histogram (top) and best growth curve fit (bottom) for the getter detector for copper activated for 30 minutes in the neutron howitzer via $^{65}Cu(n,\gamma)^{66}Cu$. (Right side) Same, but for the turbopump detector. The growth curve only includes the good beta events selected inside the green box in the 2D histograms.

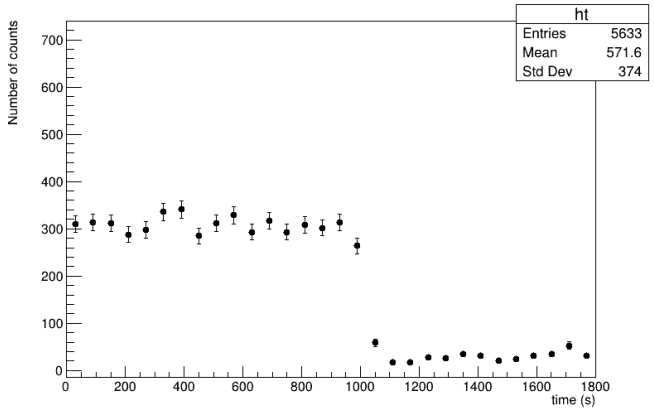

Figure 13. Total count rate as a function of time for the getter detector for copper activated for 30 minutes in the neutron howitzer via $^{65}Cu(n,\gamma)^{66}Cu$. This plot differs from Figure 12 bottom left in that it includes all events, not just those selected inside the green box. This shows that the noise pulse rate (the large peak in the lower left in Figure 12 top left) suddenly dropped at around 1000 seconds into the measurement. The reason is not known.

IV. Future Experiments for Summer 2021

At the time this report was prepared, there are still two more weeks of planned beam time for experiments. The plans for the next two weeks include:

1. **$^{65}Cu(d,p)^{66}Cu$ activation experiments.** Several experiments are planned that simply involve activating copper via $^{65}Cu(d,p)^{66}Cu$ for approximately 6 half-lives, and then looking at the emitted radiation to measure the energy spectra and decay curve. This will allow the initial activity to be measured, which is necessary to determine the fraction collected after it is evaporated.
    a. Determine the lowest energy deuterons capable of creating in the copper to the desired activity. The estimates in Table 3 are based on a 10 nA, 3 MeV beam of deuterons. Deuterons at this energy will produce significant radiation dose rates in the vicinity.
    b. Activate copper using the accelerator deuterons, then quickly transport it to a counting station where NaI detectors will be used to measure the gamma spectrum.
    c. Activate the copper, then use the getter detector, a few centimeters away in the chamber, to measure the dE-E spectrum for the emitted beta particles.

2. **Exploding wire experiments with the getter detector.** The next set of experiments will be to measure the amount of ^{65}Cu deposited onto the getter detector when the tungsten ribbon is heated and the copper is evaporated.
    a. Activate the copper and evaporate it quickly, with the shield removed. Then begin counting.
    b. Activate the copper and evaporate it quickly, with the shield removed. Then move the shield between the tungsten ribbon and the getter detector and begin counting.
    c. Activate the copper and evaporate it quickly, with the shield between the tungsten ribbon and the getter detector and begin counting.

3. **Exploding wire experiment with the turbopump detector**. This experiment will test the turbopump trap and detector. First activate the copper, then It seems likely that the copper will deposit on the tube before it reaches the detector. Nevertheless, it would be worth activating the copper, evaporating it, and looking to see if it can be detected in the turbopump trap.

4. **Teflon fluorine activation experiments.** The $^{19}F(d,p)^{20}F$ reaction could be used to produce even shorter lived products for testing the detectors, that may be less likely to stick to surfaces in the vacuum chamber than copper. The main pyrolysis products at temperatures above about 400°C are tetrafluoroethylene and difluorocarbene radicals which hopefully would quickly react to form tetrafluoroethylene.
    a. Attach very thin Teflon tape to tungsten ribbon and heat, observe pyrolysis.
    b. Activate Teflon tape using $^{19}F(d,p)^{20}F$ with deuteron beam from accelerator. Observe beta particle using getter detector.
    c. Activate Teflon tape using $^{19}F(d,p)^{20}F$, pyrolyze using tungsten ribbon, then count decays using the getter detector.
    d. Activate Teflon tape using $^{19}F(d,p)^{20}F$, pyrolyze using tungsten ribbon, then count decays using the turbopump detector.

V. Future Plans

The measurements described in Section IV will shed light on our ability to trap and detect short-lived radioactive gasses, and hopefully give an idea of what might be expected for the fraction of the product nuclei trapped. In the future, before a full-scale experiment at OMEGA, the following work still needs to be done:

1. **Short half-life measurements at Houghton College using $^{137}Cs/^{137m}Ba$ isotope generator.** Figure 14 shows a liquid feedthrough with an airlock that was built to inject a solution containing ^{137}Ba into the chamber. An ammonium acetate solution can be used, instead of the usual NaCl and hydrochloric acid solution, to elute the ^{137}Ba from a Spectrum Techniques Cs-137/Ba-137m Isotope Generator. The $CH_3CO_2NH_4$ has the advantage of not leaving salt deposits inside the vacuum chamber. The ^{137m}Ba has a 2.6 minute half-life. Although it purely undergoes gamma decay from the metastable state to the ground state, the 0.662 MeV gamma rays that are emitted can still be detected, albeit with a low efficiency and without the beta particle identification.

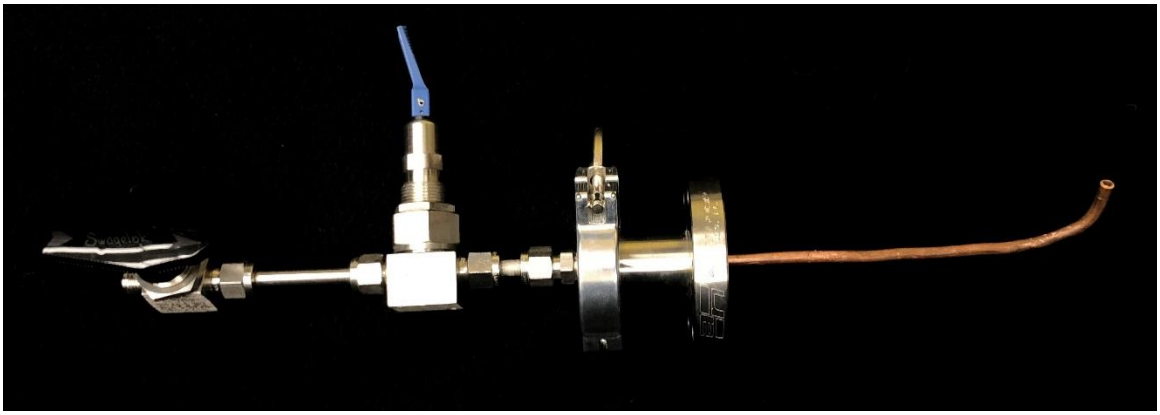

Figure 14. Airlock system to that can be used to inject a $CH_3CO_2NH_4$ containing 137mBa into the test vacuum chamber.

2. **Reduce light loss in the getter detector light guide.** The thin scintillator used in the phoswich detector produces very little light when a beta particle travels through it. The loss of 60% of the light (or more in the longer lightguide needed for the OMEGA target chamber) greatly reduces the energy resolution. We should explore:
    a. The use of small diameter fiber optics to transmit the light.
    b. The possibility of using a small diameter phototube with the phoswich detector directly attached close to target center.

3. **Construct the prototype Ion-pump trap and detector.** The third trap under consideration would use an ion-pump and a phoswich detector between the wall of the pump and the magnet.

4. **Eliminate analog signal processing and improve digitizer speed.** The high count rates that were measured directly outside the target chamber shortly after a high-yield OMEGA shot (see 2020 report [10]) indicate the need to improve the speed of the acquisition electronics. In particular, the 3.5 μs dead time due to the analog linear gates created severe pileup problems at these high rates. An all-digital system could reduce the deadtime to at most a few hundred nanoseconds by sampling and storing every 2 ns the phototube pulse. Storing a couple hundred samples of reach event would allow the fast and slow components to be reconstructed offline, even when there was significant overlap.
    a. A crowd-sourced FPGA-based acquisition board capable of sampling at this rate and with enough memory to store over 10 s of events at 100,000 events/s has been purchased. We are working with Dr. Ki Shin, a Houghton College electrical engineering professor, and a Houghton EE undergraduate, Jon Zdunski, on programing this board to operate in the desired manner. This is made difficult by the lack of documentation provided with crowd-sourcing.
    b. We have reached out to CAEN SpA to seek their advice on commercial products that might meet our need. We also contacted Wojtek Skuski, whose company, Skutek Instrumentation, makes the FemtoDAQ system we are currently using.

5. **OMEGA ride-along experiment.** Once a digital system is ready, it would make sense to have another ride-along experiment in which we test the performance of our detectors and acquisition electronics at these rates. This time we would also explore the value of shielding.

This material is based upon work supported by the Department of Energy [National Nuclear Security Administration] University of Rochester "National Inertial Confinement Program" under Award Number(s) DE-NA0004144.

[1] Loomis et al., Los Alamos National Laboratory Report LA-UR-05-0775, 2005.
[2] F.J. Wilkinson III and F.E. Cecil, Physical Review **C31**, 2036 (1985).
[3] C.A. Barnes, K.H. Chang, T.R. Donoghue and C. Rolfs, Physics Letters **B197**, 315 (1987).
[4] M. Yuly, S. Padalino, E. Bruce, K. Cook, and S. Hull. "Measuring Low Energy Nuclear Cross Sections using ICF" in Nuclear and Plasma Diagnostics for the EP-OMEGA and MTW Laser Systems, LLE proposal (2018).
[5] S.N. Abramovich, B.Ya. Guzhovskij, V.A. Zherebtsov, and A.G. Zvenigorodskij, International Nuclear Data Committee Report INDC(CCP)-326/L+F, (1991).
[6] A.J. Koning, S. Hilaire and M.C. Duijvestijn, "TALYS-1.0", Proceedings of the International Conference on Nuclear Data for Science and Technology, April 22-27, 2007, Nice, France, editors. O.Bersillon, F.Gunsing, E.Bauge, R.Jacqmin, and S.Leray, EDP Sciences, 2008, p. 211-214.
[7] M. Yuly, S. Padalino, T. Kowalewski, S. Ferri and S. Raymond. "Inertial Confinement Fusion as a Tool to Study Fundamental Nuclear Science, The rapid isotope-counting system (RICS) using a hollow box phoswich detector" in Nuclear and Plasma Diagnostics for the EP-OMEGA and MTW Laser Systems, LLE Proposal (2019)
[8] M. Yuly, S. Padalino, M. Coats and K. Cook. "A Phoswich Detector System to Measure the $^{3}H(t,\gamma)^{6}He$ Cross Section using ICF" in Nuclear and Plasma Diagnostics for the EP-OMEGA and MTW Laser Systems, LLE Proposal (2017).

[9] Mark Yuly, Stephen Padalino, Emma Bruce, Katelyn Cook, and Sarah Hull. "Measuring Low Energy Nuclear Cross Sections using ICF" in Nuclear and Plasma Diagnostics for the EP-OMEGA and MTW Laser Systems, LLE Proposal (2018).
[10] Mark Yuly, Stephen Padalino, Micah Christensen, Joshua Bowman. "Progress toward using ICF to measure light-ion nuclear cross sections" in Continuance of the Nuclear and Plasma Diagnostics for the EP-OMEGA and MTW Laser Systems, LLE Proposal (2020).